Supporting Information

Capes et al. 10.1073/pnas.1115575109

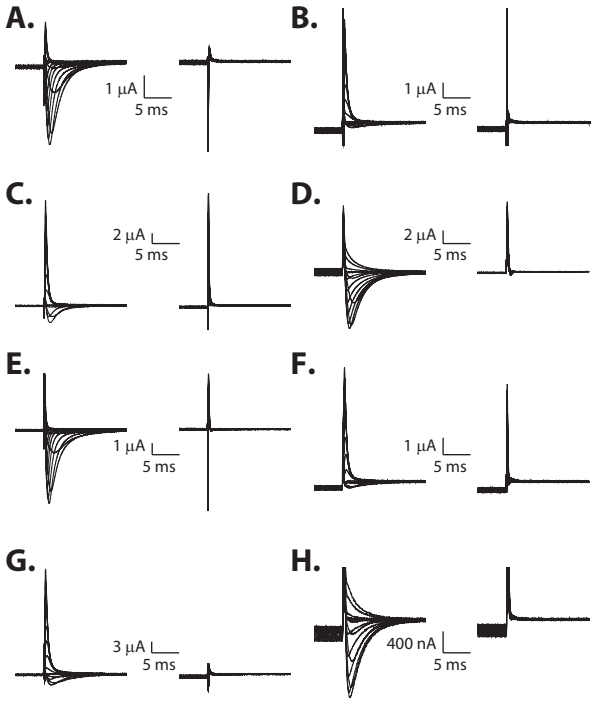

Fig. S1. Block of main pore currents by saturating concentrations of TTX or μ-CTX in the charge neutralized sodium channel mutants. Family of ionic currents elicited by depolarization before (*Left*) and after (*Right*) addition of TTX for DI-CN (*A*), DII-CN (*B*), DIII-CN (*C*), and DIV-CN (*D*). Family of ionic currents elicited by depolarization before (*Left*) and after (*Right*) addition of μ-CTX for DI-CN (*E*), DII-CN (*F*), DIII-CN (*G*), and DIV-CN (*H*). DI-CN and DIV-CN were recorded in the presence of 105 mM Na^+-Mes external solution, whereas DII-CN and DIII-CN were obtained in presence of K^+-Mes external solution. Pulse protocol is the same as reported in *Methods*.

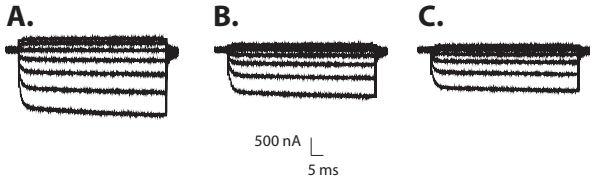

Fig. S2. Effect of increasing concentrations of TTX on DIV-CN gating pore currents. Family of DIV-CN gating pore currents before TTX addition (*A*), in 1 μM TTX (*B*), and in 10 μM TTX (*C*). Gating pore currents were recorded in the presence of 105 mM Na^+-Mes external solution. Pulse protocol is the same as reported in *Methods*.

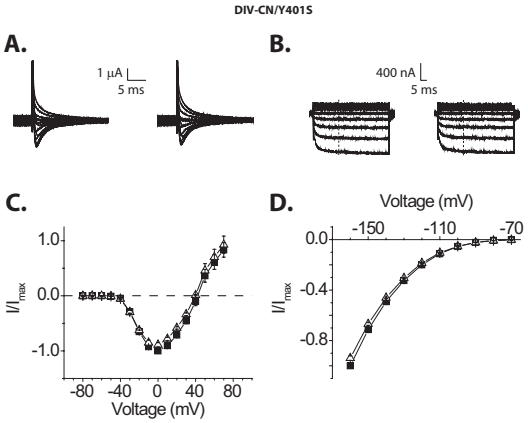

Fig. S3. TTX does not inhibit gating pore currents of the DIV-CN/Y401S mutant. (*A*) Family of DIV-CN/Y401S traces shown before (*Left*) and after (*Right*) TTX application. (*B*) Family of gating pore currents before (*Left*) and after (*Right*) addition of TTX from the DIV-CN/Y401S mutant. (*C*) Current–voltage (*I–V*) relationship of the DIV-CN/Y401S mutant in absence (unfilled triangle) and presence (filled square) of TTX. Voltage protocol is the same as in *Methods*. Data were collected in the presence of 105 mM Na^+-Mes external solution. (*D*) Normalized current–voltage plots of the gating pore currents from the DIV-CN/Y401S mutant before (filled square) and after (unfilled triangle) addition of TTX. Currents were recorded in the presence of 105 mM Na^+-Mes external solution using voltage protocols described in *Methods*. Currents were normalized to the maximum current measured before toxin, typically at −160 mV. Currents at each voltage were measured at the end of 20 ms, marked as a dashed line (*B*). Each current–voltage plot represents the mean ± SE of four experiments.

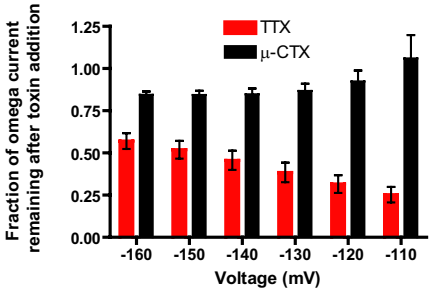

Fig. S4. Voltage dependence of TTX and μ-CTX inhibition of DIV gating pore currents. Plot of the fraction of DIV hyperpolarization-activated current remaining after toxin addition versus voltage. Each graph represents the mean ± SE of five independent experiments. Fraction of gating pore current remaining after toxin addition was calculated by dividing the currents obtained after toxin addition by the currents obtained before toxin was added (following normalization).

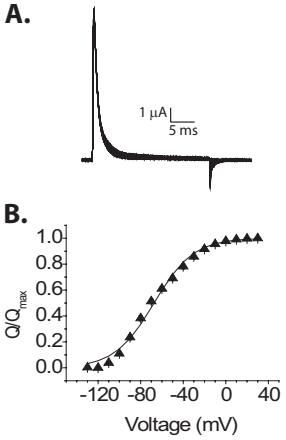

Fig. S5. (*A*) Wild-type off-gating currents in the absence of pore blocker. Voltage protocol is the same as in *Methods*. (*B*) Wild-type charge–voltage plots in the absence of pore blocker. Each plot represents the mean ± SE of 11 independent experiments.

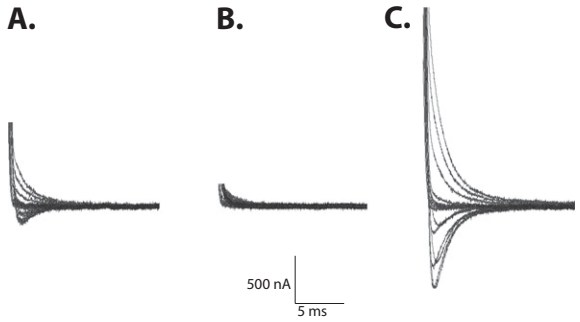

Fig. S6. Representative sodium current traces under varying redox conditions in D400C/E755C DIV-CN. Family of ionic currents from oocytes expressing the D400C/E755C DIV-CN mutant (*A*), in presence of 2 mM H_2O_2 (*B*), and upon addition of 1 mM DTT after washout of H_2O_2 (*C*). All traces were collected from the same oocyte in presence of 105 mM Na^+-Mes external solution using a voltage protocol listed in *Methods*.

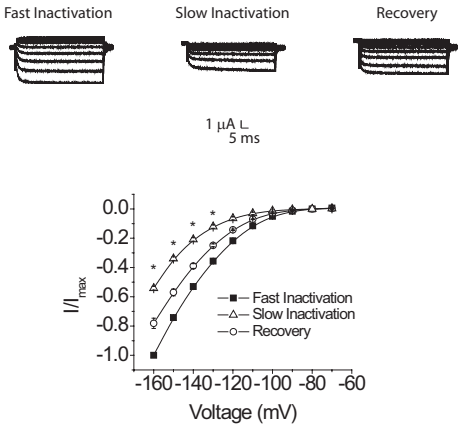

Fig. S7. Effect of cumulative slow inactivation on the DIV-CN gating pore currents. Family of gating pore currents (*Above*) is shown after fast inactivation, after a 30-s cumulative slow inactivation protocol, and after a 10-min recovery at −80 mV. Normalized current–voltage plots of the DIV-CN gating pore currents (*Below*) before slow inactivation (filled squares), after a 30-s cumulative slow inactivation protocol (unfilled triangles), and after a 10-min recovery at −80 mV (unfilled circles). The channels were pulsed from −120 mV to −10 mV for 20 ms to measure the ionic current and then a pulse train from −160–60 mV for 60 ms was collected before returning to −120 mV for 20 ms. Our cumulative inactivation protocol was modified from protocols used by Cummins and Sigworth and Townsend and Horn (1, 2). For the 30-s cumulative slow inactivation protocol, the oocytes were held at −10 mV for 30 s before beginning the protocol described above and were also held at −10 mV for 30 s in between every voltage step. Each plot represents the mean ± SE of six independent experiments. Statistical significance from the gating pore currents collected after fast inactivation, $*P < 0.02$.

1. Cummins TR, Sigworth FJ (1996) Impaired slow inactivation in mutant sodium channels. *Biophys J* 71:227–236.
2. Townsend C, Horn R (1997) Effect of alkali metal cations on slow inactivation of cardiac Na+ channels. *J Gen Physiol* 110:23–33.